

Magnetic soft x-ray microscopy of the domain wall depinning process in permalloy magnetic nanowires

Mi-Young Im¹, Lars Bocklage², Guido Meier² and Peter Fischer¹

¹ Center for X-ray Optics, Lawrence Berkeley National Laboratory, Berkeley, CA 94720, USA

² Institut für Angewandte Physik und Zentrum für Mikrostrukturforschung, Universität Hamburg, Jungiusstrasse 11, 20355 Hamburg, Germany

Abstract

Full-field magnetic transmission x-ray microscopy at high spatial resolution down to 20 nm is used to directly observe field-driven domain wall motion in notch-patterned permalloy nanowires. The depinning process of a domain wall around a notch exhibits a stochastic nature in most nanowires. The stochasticity of the domain wall depinning sensitively depends on the geometry of the nanowire such as the wire thickness, the wire width, and the notch depth. We propose an optimized design of the nanowire for deterministic domain wall depinning field at a notch.

(Some figures in this article are in colour only in the electronic version)

The propagation of magnetic domain walls (DWs) in nanowires is not only scientifically a very interesting topic, but also provides the basic concept for the novel magnetic memory and logic devices that have been proposed recently [1–3]. So far, many efforts have been dedicated to the study of current- and field-driven DW dynamics in magnetic wires to investigate the DW speed and the effective current and field to move a DW [2, 4]. In addition, numerous experimental studies focused on the DW pinning and depinning processes in geometrically designed magnetic structures such as ring- and L-shaped nanowires [5, 6]. Imaging techniques, e.g. magnetic transmission x-ray microscopy (MTXM), optical Kerr microscopies, scanning electron microscopy with polarization analysis (SEMPA), and electron holography have been extensively used to directly observe the detailed behavior of DWs and their internal structures in magnetic materials [7–10].

For the realization of DW-based devices it is essential to fully control the motion of a DW along a nanowire. Any non-deterministic DW behavior could potentially compromise the reliability of DW applications [4, 8]. Generally, a local control of the DW propagation is achieved by introducing artificial constrictions such as notches or anti-notches in

nanowires [6, 8, 11–13]. They act as pinning sites for the DW at specific locations due to their higher pinning potential compared to intrinsic pinning sites such as defects, which are mostly randomly distributed [7, 14]. Although many experimental studies have been devoted to the study of DW dynamics around an artificial constriction in a magnetic nanowire [6, 11–17], there is very little experimental evidence of the statistical behavior of the DW pinning and depinning based on sufficient statistics [8, 18–20]. Thus, the question of how a deterministic DW process can be achieved through geometric modifications is still unsolved.

Here, we report the direct observation of the statistical nature of DW depinning in notch-patterned permalloy (Py, Ni₈₀Fe₂₀) nanowires with various wire widths (w), film thicknesses (t), and notch depths (N_d). We demonstrate that an optimized geometry of the magnetic nanowire provides a deterministic DW depinning field in the vicinity of a notch.

We used magnetic full-field transmission soft x-ray microscopy (MTXM) at BL 6.1.2 at the Advanced Light Source in Berkeley, CA [21] to observe DW evolution patterns in nanowires. MTXM enables element specific imaging by selecting characteristic photon energies corresponding e.g. to Fe L₃ (706 eV), Co L₃ (778 eV), or Ni L₃ (854 eV)

absorption edges. Here, the magnetic imaging in Py nanowires was performed at the Fe L_3 absorption edge. Magnetic contrast is provided by x-ray magnetic circular dichroism (XMCD), using the dependence of the x-ray absorption coefficients on the orientation between magnetization and photon helicity [22]. Py nanowires with varying wire width ($w = 250, 450,$ and 550 nm), film thickness ($t = 30$ and 50 nm), and notch depth ($N_d \sim 0.15w, 0.3w,$ and $0.6w$) were prepared on 100 nm thick silicon-nitride membranes by electron-beam lithography and lift-off processing. To protect the structures from oxidation, they were capped by a 2 nm aluminum layer.

Figure 1(a) shows a representative TXM image of a Py nanowire. The elliptical pad is used for DW nucleation and the triangular notch serves as a pinning site. To image the in-plane configuration, the nanowires are mounted at a 30° angle between the sample's surface normal and the x-ray propagation direction. An external magnetic field applied parallel to the sample plane triggers the DW propagation along the wire. Typical field-driven DW evolution patterns measured by MTXM in a 50 nm thick wire with a width of $w = 450$ nm and a notch depth of $N_d \sim 0.3w$ are shown in figure 1(b). The wires were saturated by an external magnetic field (~ 100 mT) in the positive x -direction as indicated by the arrow in figure 1(b), and then images were recorded as the external field was successively reduced from saturation in the negative x -direction in steps of 0.5 mT. For eliminating structural contrast each image taken at a certain field step was normalized to an image measured at the saturation state. Note that an initially created DW at the elliptical pad due to lower shape anisotropy arrives at the notch. The DW is pinned at the notch until the external force by the external magnetic field exceeds the pinning force exerted by the notch. Once the DW is depinned from the notch by increasing the external field strength it finally annihilates at the narrow tip of the nanowire.

The DW depinning in particular at an artificial notch is investigated by repeated imaging of DW propagation in successive hysteretic cycles. Three pairs of DW pinning and depinning images of the wire with $w = 250,$ $t = 50$ nm, and $N_d \sim 0.3w$ are shown in figure 2(a), where the colors indicate DW pinning and depinning field strengths. It can be seen that the depinning fields around the notch are stochastic within repetitions. As a possible explanation for the stochastic nature of DW depinning fields, the thermal energy, the edge roughness, and the generation of different types of DW structures can be considered. In our previous work, we have found that the depinning fields are strongly related to the structures of DWs [8]. It has been directly observed that two types of DWs, either a transverse wall or a vortex-domain wall are generated around a notch in repeated experiments and they are depinned at different magnetic fields. The transverse wall depins at lower magnetic field than the vortex-domain wall. From the observation, we interpret that the stochastic nature of depinning fields might be due to the variety of DW types generated at the notch. It has been also reported by various studies on the stochastic behavior of the DW process in wires that the DW depinning process sensitively depends not only on the type of DW structure, but

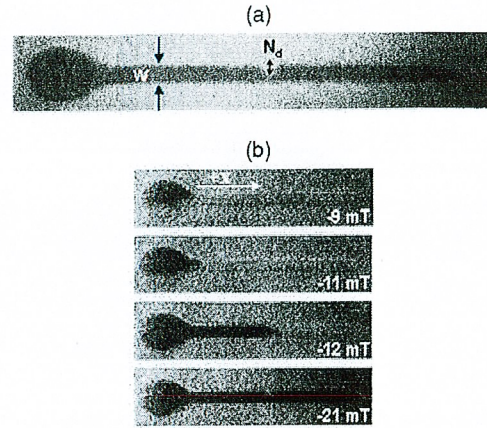


Figure 1. (a) Typical TXM image of a notch-patterned permalloy nanowire. The elliptical head and triangular notch serve as a DW nucleation pad and artificial pinning site. (b) Representative image sequence of magnetic DW evolution along the nanowire during a hysteretic cycle for the 50 nm thick wire of $w = 450$ nm and $N_d \sim 0.3w$.

also on the rotation sense of in-plane magnetization of the transverse wall and the orientation of the vortex core in the vortex-domain wall, etc [11, 19, 20]. Based on the observation that the depinning fields of DWs with unlike structures are different, the probability of the appearance of each DW structure is expected to be reflected in the distribution of depinning fields. We have also investigated the distribution of depinning fields and found that an isolated peak exists in the distribution [8], which suggests that a certain type of DW structure dominantly appears rather than the other types of structures. Although we address here that the multiplicity of DW types generated around a notch might be responsible for the stochastic nature of depinning fields, other effects such as thermal and roughness can also contribute to the stochastic nature of the DW depinning process in nanowires.

To systematically investigate the statistical behavior of DW depinning fields, we performed measurements over 40 times under identical conditions for wires with different thicknesses and widths. Figure 2(b) shows the absolute value of the averaged depinning field (m) and the standard deviation (SD, σ) of the depinning fields for the wires with different wire widths of 250 and 450 nm, which are listed in the table. The depinning field decreases as the wire widens from 250 to 450 nm, which is expected as the size of a DW at a notch depends on the wire width and the DW becomes energetically unfavorable as its size increases. Hence, a larger DW in a wider wire ($w = 450$ nm) depins at lower fields. The SD of the DW depinning fields is also considerably reduced with increasing the wire width from 250 to 450 nm. Since the SD is a measure of the DW depinning field distribution, technological applications aim for a minimal SD of the depinning field.

Experiments for wires with different notch depths were also performed. Figure 3(a) shows scanning electron microscope (SEM) images of notches with $N_d \sim 0.6w, 0.3w,$ and $0.15w$. Based on the experimental result in figure 2(b),

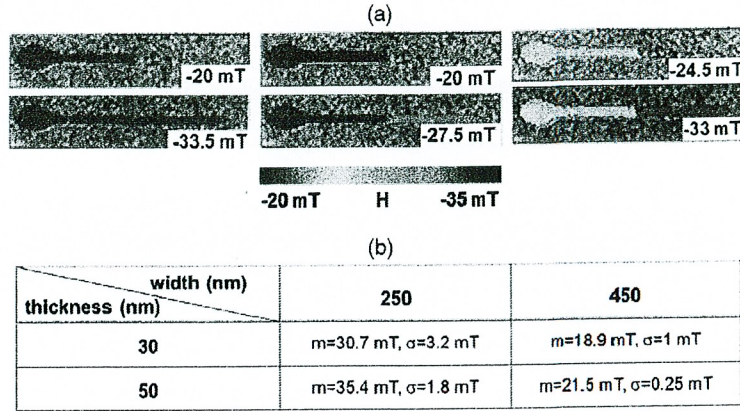


Figure 2. (a) Domain wall pinning and depinning images around the notch in the wire with $w = 250 \text{ nm}$, $t = 50 \text{ nm}$, and $N_d \sim 0.3w$. Three consecutive measurements were performed under identical experimental conditions. The color scale represents the field strength when a DW is pinned and depinned at the notch. (b) The absolute value of the averaged depinning field (m) and the standard deviation of depinning fields (σ) of the wires with different wire widths of 250 and 450 nm, which are listed in the table. The values are obtained by statistical analysis of several tens of DW depinning events in 30 and 50 nm thick nanowires with the fixed notch depth of $N_d \sim 0.3w$.

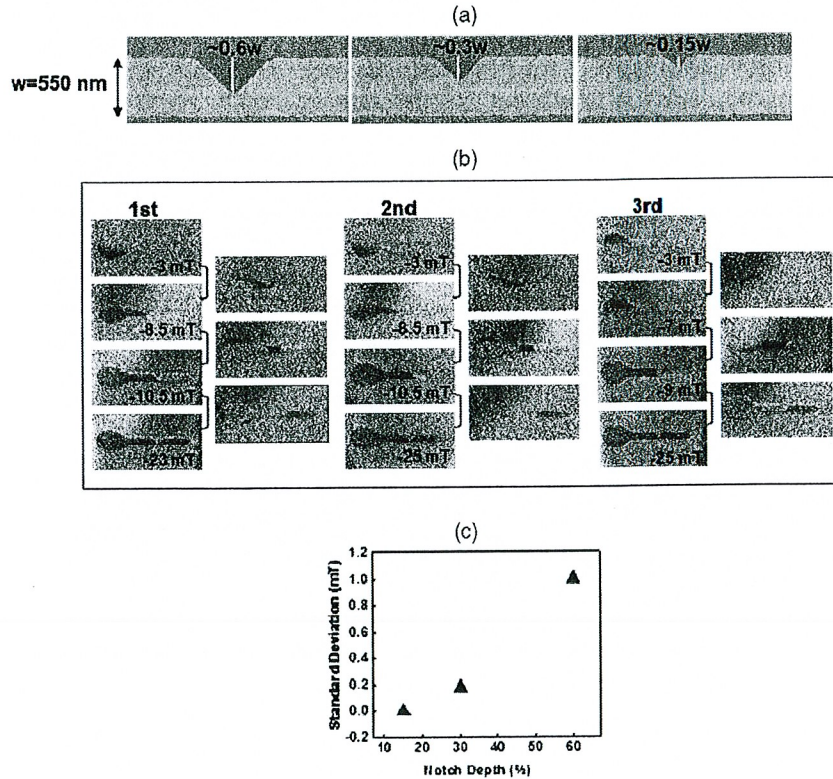


Figure 3. (a) Enlarged scanning electron microscope (SEM) images of notch patterns with the depths of $0.6w$, $0.3w$, and $0.15w$. (b) Three DW evolution images taken from successive hysteretic cycles in the wire of $w = 550 \text{ nm}$, $t = 50 \text{ nm}$, and $N_d \sim 0.6w$ together with the difference images to clearly visualize the evolution pattern in each field step. (c) Standard deviation of DW depinning fields with respect to the notch depths of $0.6w$, $0.3w$, and $0.15w$.

which reveals that SD decreases in wider and thicker wires, we chose a wire width of $w = 550 \text{ nm}$ and a thickness of $t = 50 \text{ nm}$ to minimize the SD. An image sequence of DW evolutions taken in the wire of $N_d \sim 0.6w$ by three consecutive measurements is seen in figure 3(b). Prior to reaching the notch area, the nucleated DW is pinned at

several local pinning sites. It is interesting to note that the locations of the DW nucleation and the pinning fluctuate in repeated experiments. In general, randomly distributed local pinning sites provide energy barriers comparable to thermal energies, which activate DW nucleation and propagation [7, 23]. Therefore, thermal fluctuations induce the experimentally

observed randomness of DW pinning and depinning processes from the nucleation pad to the notch. The pinning field of the DW at the notch is strongly associated with the DW nucleation and pinning processes prior to arrival at the notch. When the positions of DW nucleation and pinning as well as the DW evolution pattern are identical throughout the wire, the DW pinning fields at the notch are also identical. On the other hand, the depinning field of DWs from the notch is not directly linked to preceding DW processes and even to the DW pinning mechanism near the notch. For instance, depinning fields appear differently even for identical DW pinning fields, which suggests that the depinning process is mostly determined by complex processes in the vicinity of a notch such as the deformation of DW structures under an interaction between a DW and a notch [6].

The stochastic natures of DW depinning fields for the wires were quantitatively analyzed. Figure 3(c) shows the standard deviation of the depinning field of wires with notch depths of $N_d \sim 0.6w$, $0.3w$, and $0.15w$, where only depinning events which were accompanied by DW pinning at the notch were considered. The pinning probability of DW at a notch is found to vary from 100 to 60% as the notch shallows from $0.6w$ to $0.15w$. Interestingly, we find a SD close to zero in the wire of $N_d \sim 0.15w$. This implies that the DW depinning process is almost deterministic in this wire geometry and for our hysteresis step width. Considering that the stochasticity of the DW depinning fields in a magnetic nanowire is strongly correlated with the variety of DW types, we conclude that the deterministic DW depinning process is due to the creation of a single DW type at the notch in this suitably designed wire.

In conclusion, we have studied the DW depinning at a notch in Py wires by high resolution soft x-ray microscopy. We observe that the stochastic nature of the depinning field depends considerably on the wire width, the thickness, and the notch depth. We find that the depinning field in the wire of $w = 550$ nm, $t = 50$ nm, and $N_d \sim 0.15w$ is completely deterministic, which allows us to conclude that a proper geometrical design yields a deterministic DW depinning in notched Py nanowires.

Acknowledgments

This work was supported by the Director, Office of Science, Office of Basic Energy Sciences, of the US Department of Energy under Contract No. DE-AC02-05CH11231. Financial support of the Deutsche Forschungsgemeinschaft via the Sonderforschungsbereich 668 and the Graduiertenkolleg 1286 as well as of the Forschungs- und Wissenschaftsstiftung Hamburg via the Exzellenzcluster 'Nano-Spintronik' is gratefully acknowledged.

References

- [1] Allwood D A, Xiong G, Faulkner C C, Atkinson D, Petit D and Cowburn R P 2002 Magnetic domain-wall logic *Science* **296** 1688
- [2] Hayashi M, Thomas L, Moriya R, Rettner C and Parkin S S S 2008 Current controlled magnetic domain-wall nanowire shift register *Science* **320** 209
- [3] Cowburn R P 2007 Champing at the bit *Nature* **448** 544
- [4] Meier G, Bolte M, Eiselt R, Krüger B, Kim D H and Fischer P 2007 Direct imaging of stochastic domain-wall motion driven by nanosecond current pulses *Phys. Rev. Lett.* **98** 187202
- [5] Kläui M, Vaz C A F, Rothman J, Bland J A C, Wernsdorfer W, Faini G and Cambri E 2003 Domain wall pinning in narrow ferromagnetic ring structures probed by magnetoresistance measurements *Phys. Rev. Lett.* **90** 097202
- [6] Faulkner C C, Cooke M D, Allwood D A, Petit D, Atkinson D and Cowburn R P 2004 Artificial domain wall nanotraps in $\text{Ni}_{81}\text{Fe}_{19}$ wires *J. Appl. Phys.* **95** 6717
- [7] Im M Y, Lee S H, Kim D H, Fischer P and Shin S C 2008 Scaling behavior of the first arrival time of a random-walking magnetic domain *Phys. Rev. Lett.* **100** 167204
- [8] Im M Y, Bocklage L, Fischer P and Meier G 2009 Direct observation of stochastic domain-wall depinning in magnetic nanowires *Phys. Rev. Lett.* **102** 147204
- [9] Gavrin A and Unguris J 2000 SEMPA imaging of domain dynamics in amorphous metals *J. Magn. Mater.* **213** 95
- [10] He K, Smith D J and McCartney M R 2009 Observation of asymmetrical pinning of domain walls in notched permalloy nanowires using electron holography *Appl. Phys. Lett.* **95** 182507
- [11] Hayashi M, Thomas L, Rettner C, Moriya R, Jiang X and Parkin S S P 2006 Dependence of current and field driven depinning of domain walls on their structure and chirality in permalloy nanowires *Phys. Rev. Lett.* **97** 207205
- [12] Bocklage L, Krüger B, Matsuyama T, Bolte M, Merkt U, Pfannkuche D and Meier G 2009 Dependence of magnetic domain-wall motion on a fast changing current *Phys. Rev. Lett.* **103** 197204
- [13] Kläui M *et al* 2005 Direct observation of domain-wall pinning at nanoscale constrictions *Appl. Phys. Lett.* **87** 102509
- [14] Herrmann M, McVitie S and Chapman J N 2000 Investigation of the influence of edge structure on the micromagnetic behavior of small magnetic elements *J. Appl. Phys.* **87** 2994
- [15] Kleemann W, Rhensius J, Petravic O, Ferré J and Jamet J P 2007 Modes of periodic domain wall motion in ultrathin ferromagnetic layers *Phys. Rev. Lett.* **99** 097203
- [16] Yokoyama Y *et al* 2000 Kerr microscopy observations of magnetization process in microfabricated ferromagnetic wires *J. Appl. Phys.* **87** 5618
- [17] Thomas L, Rettner C, Hayashi M, Samant M G, Parkin S S P, Doran A and Scholl A 2005 Observation of injection and pinning of domain walls in magnetic nanowires using photoemission electron microscopy *Appl. Phys. Lett.* **87** 262501
- [18] Vogel A *et al* 2010 Domain-wall pinning and depinning at soft spots in magnetic nanowires *IEEE Trans. Magn.* **40** 461708
- [19] Briones J, Montaigne F, Hehn M, Lacour D, Childress J R and Carey M J 2011 Stochastic and complex depinning dynamics of magnetic domain walls *Phys. Rev. B* **83** 060401
- [20] Akerman J, Muñoz M, Maicas M and Prieto J L 2010 Stochastic nature of the domain wall depinning in permalloy magnetic nanowires *Phys. Rev. B* **82** 064426
- [21] Fischer P, Kim D H, Chao W, Liddle J A, Anderson E H and Attwood D T 2006 Soft x-ray microscopy of nanomagnetism *Mater. Today* **9** 26
- [22] Chen C T, Sette F, Ma Y and Modesti S 1990 Soft x-ray magnetic circular dichroism at the $L_{2,3}$ edges of nickel *Phys. Rev. B* **42** 7262
- [23] Martinez E, Lopez-Diaz L, Alejos O, Torres L and Tristan C 2007 Thermal effects on domain wall depinning from a single notch *Phys. Rev. Lett.* **98** 267202

DISCLAIMER

This document was prepared as an account of work sponsored by the United States Government. While this document is believed to contain correct information, neither the United States Government nor any agency thereof, nor The Regents of the University of California, nor any of their employees, makes any warranty, express or implied, or assumes any legal responsibility for the accuracy, completeness, or usefulness of any information, apparatus, product, or process disclosed, or represents that its use would not infringe privately owned rights. Reference herein to any specific commercial product, process, or service by its trade name, trademark, manufacturer, or otherwise, does not necessarily constitute or imply its endorsement, recommendation, or favoring by the United States Government or any agency thereof, or The Regents of the University of California. The views and opinions of authors expressed herein do not necessarily state or reflect those of the United States Government or any agency thereof or The Regents of the University of California.